*Inorg. Chem.* **2008**, *47*, 7775−7783

# Interconversion between (3,1) and (4,0) Isomers of $Ru_2(L)_4X$ Complexes where L is 2-Anilinopyridinate or 2-(2,4,6-Trifluoroanilino)pyridinate Anion and X = $Cl^-$ or $C{\equiv}CC_5H_4N^-$

**Minh Nguyen,[†] Tuan Phan,[‡] Eric Van Caemelbecke,[†,§] Wiroaj Kajonkijya,[†] John L. Bear,*[,†] and Karl M. Kadish*[,†]**

*Department of Chemistry, University of Houston, Houston, Texas 77204-5003, Department of Chemistry, Texas Southern University, Houston, Texas 77004, and Houston Baptist University, 7502 Fondren Road, Houston, Texas 77074-3298*

Received April 30, 2008

A reaction between the (4,0) isomer of $Ru_2(ap)_4Cl$ and $LiC{\equiv}CC_5H_4N$ leads to a (3,1) isomer of $Ru_2(ap)_4(C{\equiv}CC_5H_4N)_2$ **1** (ap = anilinopyridinate anion), whereas a reaction involving the (3,1) isomer of $Ru_2(F_3ap)_4Cl$ and $TBACl \cdot H_2O$ leads to (4,0) $Ru_2(F_3ap)_4Cl$ **2** ($F_3ap$ = 2-(2,4,6-trifluoroanilino)pyridinate anion). To our knowledge, these are the first documented examples for isomeric conversion involving diruthenium compounds with tetracarboxylate-type structures. The structural, electrochemical, and spectroscopic properties of **1** and **2** were examined. The reversible $Ru_2^{5+/6+}$ process of (3,1) $[Ru_2(F_3ap)_4Cl]^+$ is located at 0.62 V in $CH_2Cl_2$, 0.1 M TBAP but shifts to 0.29 V upon formation of (3,1) $Ru_2(F_3ap)_4Cl_2$ in $CH_2Cl_2$ containing chloride from added $TBACl \cdot H_2O$ and shifts even further to $E_{1/2}$ = 0.10 V after generation of (4,0) $Ru_2(F_3ap)_4Cl_2$ in solution. The 190 mV potential difference between the $Ru_2^{6+/5+}$ redox couples of (3,1) $Ru_2(F_3ap)_4Cl_2$ and (4,0) $Ru_2(F_3ap)_4Cl_2$ in chloride-containing media can be compared to a smaller potential difference of only 60 mV between the $Ru_2^{6+/5+}$ redox couples of (3,1) $Ru_2(F_3ap)_4Cl$ and (4,0) $Ru_2(F_3ap)_4Cl$ in $CH_2Cl_2$ containing 0.1 M tetrabutylammonium perchlorate (TBAP) as supporting electrolyte. The larger $\Delta E_{1/2}$ in the case of the bis-chloride complexes in solutions containing 0.1 M $TBACl \cdot H_2O$ can be accounted for in large part by structural differences that manifest themselves in different strengths of axial coordination to the $Ru_2^{5+}$ form of the compounds.

## Introduction

A large number of diruthenium and dirhodium complexes with tetracarboxylate-type structures with symmetrical, unsymmetrical, or mixed anionic bridging ligands have been synthesized and characterized as to their structural and physicochemical properties.[1–48] Compounds of the type $M_2L_4$ where M = Ru or Rh, L is an anilinopyridinate (ap) or substituted anilinopyridinate anion may exist in up to four different isomeric forms, which are represented as the (4,0), (3,1), (2,2)-cis, and (2,2)-trans conformations schematically shown in Chart 1 for the case of the $Ru_2^{5+}$ derivatives.

Approximately, half of the structurally characterized diruthenium and dirhodium complexes synthesized in our laboratory over the last 25 years with four identical unsymmetrical bridging ligands have been isolated as a mixture of several isomers, the most common of which possessed (4,0) and (3,1) configurations that seem to be synthetically favored. The other half of the structurally characterized compounds were isolated only in a single isomeric form, again either (4,0) or (3,1) but not both.

Numerous $M_2(L)_4$ complexes with ap or substituted-ap bridging ligands have also been examined in our laboratory over the years as to their reactivity with small molecules,[14,21–24,30,32,35,37,41,42,45] examples of which include NO,[45] CO,[35] $C{\equiv}CC_6H_5^-$,[23,30] $[C{\equiv}C{-}C{\equiv}C{-}Si(CH_3)_3]^-$,[14]

* To whom correspondence should be addressed. E-mail: kkadish@uh.edu.
† University of Houston.
‡ Texas Southern University.
§ Houston Baptist University.

(1) Ying, J.-W.; Cordova, A.; Ren, T. Y.; Xu, G.-L.; Ren, T. *Chem.—Eur. J.* **2007**, *13*, 6874.
(2) Chen, W.-Z; Fanwick, P. E.; Ren, T. *Organometallics* **2007**, *26*, 4115.
(3) Chen, W.-Z; Protasiewicz, J. D.; Davis, S. A.; Updegraff, J. B.; Ma, L.-Q.; Fanwick, P. E.; Ren, T. *Inorg. Chem.* **2007**, *46*, 3775.
(4) (a) Cotton, F. A.; Lin, C.; Murillo, C. A *Acc. Chem. Res.* **2001**, *34*, 759. (b) Cotton, F. A.; Lin, C.; Murillo, C. A. *Proc. Natl. Acad. Sci., U.S.A.* **2002**, *99*, 4810.

10.1021/ic800787p CCC: $40.75 
Published on Web 08/01/2008

$CN^-$,[21,24] or $NCN^{2-}$.[22] In each case, the isomeric configuration of the parent $M_2(L)_4$ complex was retained after formation of the axially coordinated compound and this was true independent of the nature of the anionic bridging ligand(s), the axial ligands, or the dimetal oxidation state, which, in the case of diruthenium, was usually $Ru_2^{6+}$, $Ru_2^{5+}$, or $Ru_2^{4+}$ in the final reaction product. Although, different isomers were obtained upon changing the solvent of crystallization for $Os_2(ap)_4Cl_2$,[49] to the best of our knowledge there have been no reports in the literature where the binding of an axial ligand to $Ru_2(L)_4$ or $Rh_2(L)_4$ would trigger a change in its isomeric form, that is, a conversion of a (4,0) isomer to a (3,1) isomer or vice-versa. Thus, we were recently surprised to observe two different examples of isomeric transformations while examining the ligand binding reactivity of (4,0) $Ru_2(ap)_4Cl$ and (3,1) $Ru_2(F_3ap)_4Cl$. One transformation involved a (4,0) to a (3,1) isomeric conversion of $Ru_2(ap)_4Cl$ and the other a (3,1) to (4,0) isomeric conversion of $Ru_2(F_3ap)Cl$. It was believed that only the (4,0) isomer of $Ru_2(ap)_4Cl$ could be synthesized,[12] and thus the possibility for synthesizing or isolating $Ru_2(ap)_4Cl$ in any isomeric form other than (4,0) had not previously been suggested. In contrast, (3,1) $Ru_2(F_3ap)_4Cl$ is synthesized as a mixture of the (4,0) and (3,1) isomers. These can then be separated (with some difficulty), but a conversion between the two isomeric forms of the compound has never been observed to occur after isolation of a given $Ru_2(F_3ap)_4Cl$ compound in an isomerically pure form. Thus, our observations of these transformations, which are described in the present article, were totally unexpected and might provide insights into the synthesis of other known tetracarboxylate-type diruthenium complexes in previously unreported isomeric forms. Both isomeric conversions, that is, (4,0) to (3,1) and (3,1) to (4,0), are described in the present article and a structural, electrochemical, and spectroscopic characterization of the reaction products is presented.

**Chart 1**

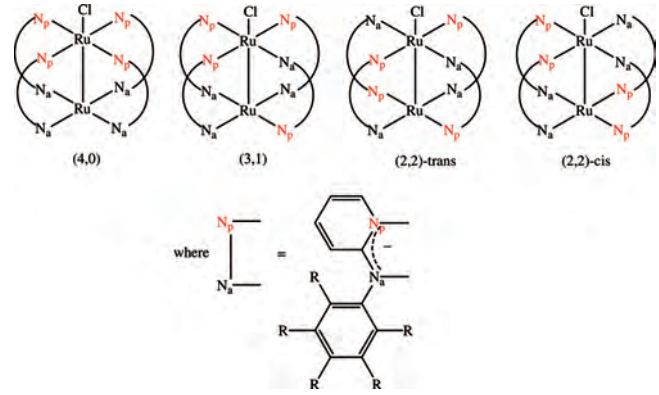


## Experimental Section

**Chemicals and Reagents.** Ultra-high purity nitrogen was purchased from Matheson-Trigas. GR graded dichloromethane, diethyl ether, ethyl acetate, and absolute dichloromethane (for electrochemical and UV−vis spectroelectrochemical measurements), from EMD, VWR, Fluka or Aldrich, tetra-*n*-butylammonium chloride monohydrate (TBACl·$H_2O$) from J. T. Baker and tetraethylammonium chloride (TEACl) from Sigma were used as


(5) (a) Barral, M. C.; Gallo, T.; Herrero, S.; Jimenez-Aparicio, R.; Torres, M. R.; Urbanos, F. A. *Chem.—Eur. J.* **2007**, *13*, 10088–10095. (b) Barral, M. C.; Gonzalez-Prieto, R.; Jimenez-Aparicio, R.; Priego, J. L.; Torres, M. R.; Urbanos, F. A. *Eur. J. Inorg. Chem.* **2006**, *21*, 4229–4232. (c) Barral, M. C.; Gonzalez-Prieto, R.; Jimenez-Aparicio, R.; Priego, J. L.; Torres, M. R.; Urbanos, F. A. *Inorgan. Chim. Acta* **2005**, *358*, 217–221. (d) Barral, M. C.; Gonzalez-Prieto, R.; Jimenez-Aparicio, R.; Priego, J. L.; Torres, M. R.; Urbanos, F. A. *Eur. J. Inorg. Chem.* **2004**, *22*, 4491–4501.

(6) Wong, K.-T.; Lehn, J.-M.; Peng, S.-M.; Lee, G.-H. *Chem. Commun.* **2000**, 2259.

(7) (a) Xu, G.-L.; Ren, T. *Inorg. Chem.* **2006**, *45*, 10431–10438. (b) Ying, J.-W.; Ren, T. *J. Organomet. Chem.* **2008**, 1449–1454.

(8) Cotton, F. A.; Herrero, S.; Jimenez-Aparcio, R.; Murillo, C. A.; Urbanos, F. A.; Villagran, D.; Wang, X. *J. Am. Chem. Soc.* **2007**, *129*, 12666–12667.

(9) (a) Miyasaka, H.; Campos-Fernández, C. S.; Clérac, R.; Dunbar, K. R. *Angew. Chem.; Int. Ed. Engl.* **2000**, *39*, 3831. (b) Miyasaka, H.; Izawa, T.; Takahashi, N.; Yamashita, M.; Dunbar, K. R. *J. Am. Chem. Soc.* **2006**, *128*, 11358–11359. (c) Miyasaka, H.; Izawa, T.; Takaishi, S.; Sugimoto, K.; Sugiura, K.; Yamashita, M. *Bull. Chem. Soc. Jpn.* **2006**, *79*, 612–620.

(10) Miyasaka, H.; Clérac, R.; Campos-Fernández, C. S.; Dunbar, K. R. *Inorg. Chem.* **2001**, *40*, 1663.

(11) (a) Zuo, J.-L; Herdtweck, E.; Kühn, F. E. *J. Chem. Soc., Dalton Trans.* **2002**, 1244. (b) Zuo, J.-L; Herdtweck, E.; Biani, F. F. D.; Santos, A. M.; Kühn, F. E *New J. Chem.* **2002**, *26*, 889. (c) Zuo, J.-L; Biani, F. F. D.; Santos, A. M.; Köhler, K.; Kühn, F. E. *Eur. J. Inorg. Chem.* **2003**, 449.

(12) Angaridis, P. In *Multiple Bonds between Metal Atoms*, 3rd edition; Cotton, F. A., Murillo, C. A., Walton, R. A., Eds.; Springer Science and Business Media, Inc.: New York, 2005; *Chapter 9.*

(13) (a) Arribas, G.; Barral, M. C.; Gonzalez-Prieto, R.; Jimenez-Aparicio, R.; Priego, J. L.; Torres, M. R.; Urbanos, F. A. *Inorg. Chem.* **2005**, *44*, 5770–5777. (b) Dikarve, E. V.; Filatov, A. S.; Clerac, R.; Petrukhina, M. A. *Inorg. Chem.* **2006**, *45*, 744–751. (c) Xi, B.; Xu, G.-L.; Ying, J.-W.; Han, H.-L.; Cordova, A.; Ren, T. *J. Organomet. Chem.* **2008**, 1656–1663. (d) Burchell, T. J.; Cameron, T. S.; Macartney, D. H.; Thompson, L. K.; Aquino, M. A. S. *Eur. J. Inorg. Chem.* **2007**, *25*, 4021–4027.

(14) Bear, J. L.; Han, B.; Wu, Z.; Caemelbecke, E. V.; Kadish, K. M. *Inorg. Chem.* **2001**, *40*, 2275.

(15) Ren, T.; Xu, G. *Comments Inorg. Chem.* **2002**, *23*, 355.

(16) Ren, T.; Zou, G.; Alvarez, J. C. *Chem. Commun.* **2000**, 1197.

(17) Miller, J. S.; Manson, J. L. *Acc. Chem. Res.* **2001**, *34*, 563.

(18) Liao, Y.; Shum, W. W.; Miller, J. S. *J. Am. Chem. Soc.* **2002**, *124*, 9336.

(19) Yoshioka, D.; Mikuriya, M.; Handa, M. *Chem. Lett.* **2002**, 1044.

(20) Zhang, L.-Y.; Chen, J.-L.; Shi, L.-X.; Chen, Z.-N. *Organometallics* **2002**, *21*, 5919.

(21) Bear, J. L.; Li, Y.; Cui, J.; Han, B.; Caemelbecke, E. V.; Phan, T.; Kadish, K. M. *Inorg. Chem.* **2000**, *39*, 857.

(22) Bear, J. L.; Li, Y.; Han, B.; Van Caemelbecke, E.; Kadish, K. M. *Inorg. Chem.* **2001**, *40*, 182.

(23) Bear, J. L.; Li, Y.; Han, B.; Van Caemelbecke, E.; Kadish, K. M. *Inorg. Chem.* **1997**, *36*, 5449.

(24) Bear, J. L.; Chen, W.-Z.; Han, B.; Huang, S.; Wang, L.-L.; Thuriere, A.; Van Caemelbecke, E.; Kadish, K. M.; Ren, T. *Inorg. Chem.* **2003**, *42*, 6230.

(25) Campos-Fernández, C. S.; Thomson, L. M.; Galan-Mascaros, J. R.; Xiang, O.; Dunbar, K. R. *Inorg. Chem.* **2002**, *41*, 1532.

(26) Chen, W.-Z.; Ren, T. *Organometallics* **2005**, *24*, 2660.

(27) Chen, W.-Z.; Ren, T. *Inorg. Chem.* **2003**, *42*, 8847.

(28) Cotton, F. A.; Stiriba, S.-E.; Yokochi, A. *J. Organomet. Chem.* **2000**, *595*, 300.

(29) Kuehn, F. E.; Zuo, J.-L.; Biani, F. F. D.; Santos, A. M.; Zhang, Y.; Zhao, J.; Sandulache, A.; Herdtweck, E. *New. J. Chem.* **2004**, *28*, 43.

(30) Kadish, K. M.; Phan, T. D.; Wang, L.-L.; Giribabu, L.; Thuriere, A.; Wellhoff, J.; Huang, S.; Van Caemelbecke, E.; Bear, J. L. *Inorg. Chem.* **2004**, *43*, 4825.

(31) Xu, G.; Ren, T. *J. Organomet. Chem.* **2002**, *655*, 239.

(32) Kadish, K. M.; Nguyen, M.; Van Caemelbecke, E.; Bear, J. L. *Inorg. Chem.* **2006**, *45*, 5996.

(33) Ren, T.; Parish, D. A.; Xu, G.-L.; Moore, M. H.; Deschamps, J. R.; Ying, J.-W.; Pollack, S. K.; Schull, T. L.; Shashidhar, R. *J. Organomet. Chem.* **2005**, *690*, 4734.

(34) Ren, T. *Organometallics* **2005**, *24*, 4854.

received. Tetra-*n*-butylammonium perchlorate (TBAP) purchased from Fluka was recrystallized from ethyl alcohol and stored in a vacuum oven at 40 °C for a few weeks prior to use. 2-(2,4,6-trifluoroaniline), ($C_6H_4NF_3$), 2-bromopyridine ($C_5H_4BrN$), 4-ethynylpyridine hydrochloride ($C_7H_5N \cdot HCl$), lithium chloride (LiCl), methyl lithium ($CH_3Li$), ruthenium chloride hydrate ($RuCl_3 \cdot 3H_2O$), and $CDCl_3$ (99.8% atom in D for NMR measurements) were purchased from Aldrich and used without additional purification. Silica gel (Merck 230−400, mesh 60 Å) was purchased from Sorbent Technologies, Inc. and used as received. $Ru_2(ap)_4Cl$ and the (3,1) isomer of $Ru_2(F_3ap)_4Cl$ were synthesized as described in the literature.[41]

**Physical Measurements.** Cyclic voltammetry and rotating disk voltammetry were carried out with an EG&G model 263A potentiostat/galvanostat. A Pine Instrument model AFMSR rotator was used to control the rotation rate of the RDE. A three-electrode system was used for all electrochemical measurements and consisted of a glassy carbon or platinum disk working electrode, a platinum wire auxiliary electrode, and a homemade saturated calomel electrode (SCE) as the reference electrode. The SCE was separated from the bulk of the solution by a fritted-glass bridge of low porosity containing the solvent/supporting electrolyte mixture. All potentials are referenced to the SCE, and measurements were carried out at room temperature. UV−vis spectroelectrochemical experiments were performed with a homemade spectroelectrochemical thin-layer cell[50] and a Hewlett-Packard model 8453 diode array spectrophotometer.

$^1H$ NMR measurements were recorded at room temperature on a General Electric QE-300 Plus spectrometer and were referenced to tetramethylsilane (TMS). Mass spectra were obtained with an Applied Biosystem Voyager DE-STR MALDI-TOF mass spectrometer equipped with a nitrogen laser (337 nm) at the University of Houston Mass Spectrometry Laboratory. Elemental analysis was carried out by Atlantic Microlab, Inc., GA.

**Synthesis of (3,1) $Ru_2(ap)_4(C{\equiv}CC_5H_4N)_2$ 1.** Into a three-neck round-bottom flask, 4-ethynyl pyridine·HCl (0.14 g, 1.00 mmole) was added and stirred under a nitrogen atmosphere at room temperature. Degassed THF was then introduced and the mixture was placed in an ice-bath at a temperature close to 0 °C for 10 min prior to adding dropwise 1.6 M MeLi (2 mL) as the solution color changed from green to purple. The solution was stirred for another 30 min prior to adding $Ru_2(ap)_4Cl$ (0.91 g, 0.100 mmole), then gradually brought to room temperature and stirred overnight, after which the solvent was removed and the crude product extracted with ethyl acetate and water (1:1 v/v). The organic layer was then concentrated and subjected to silica gel column chromatography using acetone:hexanes (1:1 v/v) as eluent. A blue band was observed and collected to yield the title compound with a 70% yield ($R_f$ = 0.4). $^1H$ NMR (300 MHz, $CDCl_3$, 20 °C, $\delta$): 8.4 (dd, 4H), 8.3 (dd, 4H), 7.3 (m, 4H), 7.1 (m, 16H), 6.9 (m, 4H), 6.7 (m, 4H), 6.4 (m, 4H), 6.3 (m, 4H). Mass spectral data [*m*/*e*, (fragment)]: 1083.4 $[Ru_2(ap)_4(C{\equiv}CC_5H_4N)_2]^+$, 982 $[Ru_2(ap)_4(C{\equiv}CC_5H_4N)]^+$, 915.2 $[Ru_2(ap)_3(C{\equiv}CC_5H_4N)_2]^+$, 879.3 $[Ru_2(ap)_4]^+$. Anal. Calcd for $C_{58}H_{44}N_{10}Ru_2$: C, 64.31; H, 4.09; N, 12.93. Found: C, 64.25; H, 4.41; N, 12.21. UV−vis spectrum in $CH_2Cl_2$: $\lambda_{max}$, nm ($\epsilon \times 10^{-3}$, $M^{-1}$ $cm^{-1}$): 607 (8.9) 1040 (2.4). IR: $\nu_{C\equiv C}$ = 2076 $cm^{-1}$.

**Synthesis of (4,0) $Ru_2(F_3ap)_4Cl$ 2.** The title compound was prepared by mixing the (3,1) isomer of $Ru_2(F_3ap)_4Cl$ with $TBACl \cdot H_2O$ in a 1:1000 molar ratio in $CH_2Cl_2$ at room temperature for 18 h. The solvent was evaporated and the brown slurry crude product was dissolved in $Et_2O$ before being extracted with water. The organic layer was collected and concentrated down to give a residue which was subjected to silica gel column chromatography using acetone as eluent. The solvent was then removed, and the brown green title compound was recovered in 95% yield. The spectral properties of the compound are identical to what has been previously reported for (4,0) $Ru_2(F_3ap)_4Cl$.[41]

**X-ray Crystallography of (3,1) $Ru_2(ap)_4(C{\equiv}CC_5H_4N)_2$ 1 and (4,0) $Ru_2(F_3ap)_4Cl$ 2.** Single-crystal X-ray crystallographic studies were performed at the University of Houston X-ray Crystallographic Center. Single crystals of (3,1) $Ru_2(ap)_4(C{\equiv}CC_5H_4N)_2$ were obtained by slow diffusion of acetone in hexanes. Single crystals of (4,0) $Ru_2(F_3ap)_4Cl$ were formed by slow diffusion of dichloromethane in hexanes, and all collected data agree within experimental error with what has been reported in the literature.[41]

All X-ray data measurements of **1** were made with a Siemens SMART platform diffractometer equipped with a 1K CCD area detector. A hemisphere of data (1271 frames at a 5 cm detector distance) was collected using a narrow-frame method with scan widths of 0.30% in omega and an exposure time of 30 s/frame. The first 50 frames were remeasured at the end of data collection to monitor instrument and crystal stability, and the maximum correction on $I$ was <1%. The data were integrated using the Siemens *SAINT* program, with the intensities corrected for Lorentz factor, polarization, air absorption, and absorption due to variation in the path length through the detector faceplate. A psi scan absorption correction was applied based on the entire data set. Redundant reflections were averaged. Final cell constants were refined using 4191 reflections having $I > 10/s$ ($I$), and these, along with other information pertinent to data collection and refinement, are listed in Table 1. The Laue symmetry was determined to be 2/*m*, and from the systematic absences noted the space group was shown unambiguously to be $P2_1/n$. The two terminal pyridine acetylide groups were found to be disordered over two slightly different orientations, and this was treated by refinement of ideal pyridine rings at each location.


(35) Kadish, K. M.; Phan, T. D.; Giribabu, L.; Shao, J.; Wang, L.-L.; Thuriere, A.; Van Caemelbecke, E.; Bear, J. L. *Inorg. Chem.* **2004**, *43*, 1012.
(36) Han, B.; Shao, J.; Ou, Z.; Phan, T. D.; Shen, J.; Bear, J. L.; Kadish, K. M. *Inorg. Chem.* **2004**, *43*, 7741.
(37) Cotton, F. A.; Murillo, C. A.; Reibenspies, J. H.; Villagran, D.; Wang, X.; Wilkinson, C. C. *Inorg. Chem.* **2004**, *43*, 8373.
(38) Angaridis, P.; Cotton, F. A.; Murillo, C. A.; Villagran, D.; Wang, X. *Inorg. Chem.* **2004**, *43*, 8290.
(39) Xu, G.-L.; Jablonski, C. G.; Ren, T. *Inorg. Chim. Acta* **2003**, *343*, 387.
(40) Xu, G.-L.; Jablonski, C. G.; Ren, T. *J. Organomet. Chem.* **2003**, *683*, 388.
(41) Kadish, K. M.; Wang, L.-L.; Thuriere, A.; Van Caemelbecke, E.; Bear, J. L. *Inorg. Chem.* **2003**, *42*, 834.
(42) Kadish, K. M.; Wang, L.-L.; Thuriere, A.; Giribabu, L.; Garcia, R.; Van Caemelbecke, E.; Bear, J. L. *Inorg. Chem.* **2003**, *42*, 8309.
(43) Hurst, S. K.; Xu, G.-L.; Ren, T. *Organometallics* **2003**, *22*, 4118.
(44) Xu, G.; Campana, C.; Ren, T. *Inorg. Chem.* **2002**, *41*, 3521.
(45) Bear, J. L.; Wellhoff, J.; Royal, G.; Van Caemelbecke, E.; Eapen, S.; Kadish, K. M. *Inorg. Chem.* **2001**, *40*, 2282.
(46) Yoshioka, D.; Mikuriya, M.; Handa, M. *Chem. Lett.* **2002**, 1044.
(47) (a) Murray, A. H.; Yue, Z.; Wallbank, A. I.; Cameron, T. S.; Vadavi, R.; MacLean, B. J.; Aquino, M. A. S. *Polyhedron* **2008**, *27*, 1270–1279. (b) Barral, M. C.; Gallo, T.; Herrero, S.; Jimenez-Aparicio, R.; Torres, M. R.; Urbanos, F. *Chem.—Eur. J.* **2007**, *13*, 10088–10095. (c) Barral, M. C.; Gallo, T.; Herrero, S.; Jimenez-Aparicio, R.; Torres, M. R.; Urbanos, F. A *Inorg. Chem.* **2006**, *45*, 3639.
(48) Barral, M. C.; Gonzalez-Prieto, R.; Herrero, S.; Jimenez-Aparicio, R.; Priego, J. L.; Royer, E. C.; Torres, M. R.; Urbanos, F. A. *Polyhedron* **2004**, *23*, 2637.
(49) Shi, Y. H.; Chen, W. Z.; John, K. D.; Da Re, R. E.; Cohn, J. L.; Xu, G. L.; Eglin, J. L.; Sattelberger, A. P.; Hare, C. R.; Ren, T. *Inorg. Chem.* **2005**, *44*, 5719.

**Table 1.** Crystal Data, Data Collection, and Processing Parameters for (3,1) $Ru_2(ap)_4(C{\equiv}CC_5H_4N)_2$ **1**

| | |
|---|---|
| compound | $Ru_2(ap)_4(C{\equiv}CC_5H_4N)_2$ **1** |
| mol formula | $C_{58}H_{44}N_{10}Ru_2$ |
| fw (g/mol) | 1083.17 |
| space group | $P2_1/n$ |
| cell constant | |
| $a$ (Å) | 10.6816(7) |
| $b$ (Å) | 19.1358(13) |
| $c$ (Å) | 23.4822(16) |
| α (deg) | 90 |
| $\beta$ (deg) | 98.163(1) |
| $\gamma$ (deg) | 90 |
| $V$ (Å$^3$) | 4751.2(6) |
| $Z$ | 4 |
| $\rho_{calcd}$ (g/cm$^3$) | 1.514 |
| $\mu$ (mm$^{-1}$) | 0.688 |
| $\lambda$(Mo Kα) (Å) | 0.71073 |
| temp (K) | 223(2) |
| R ($F_o$)[a] | 0.0650 |
| $R_w$ ($F_o$)[b] | 0.0340 |

[a] $R = \sum|F_o| - |F_c|/\sum|F_c|$. [b] $R_w = [\sum_w(|F_o| - |F_c|)^2/\sum_w|F_o|^2]^{1/2}$.

## Results and Discussion

**Synthesis.** The complex $Ru_2(ap)_4(C{\equiv}CC_5H_4N)_2$ **1** was prepared by reacting 4-ethynylpyridine hydrochloride with $CH_3Li/Et_2O$ prior to mixing with (4,0) $Ru_2(ap)_4Cl$ as shown in eq 1.

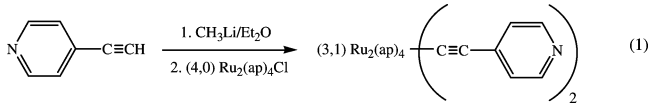


(1)

After $Ru_2(ap)_4Cl$ was allowed to react with the pyridyl acetylide anion, the solution was exposed to air and the color changed from brown-purple to deep blue. A blue product was previously observed upon air oxidation of the related $Ru_2^{6+}$ complexes, $Ru_2(L)_4(C{\equiv}CC_6H_5)_2$ (L = 2-Fap, 2,3-$F_2$ap, 2,4-$F_2$ap, 2,5-$F_2$ap, or 2,4,6-$F_3$ap),[30] thus suggesting that air oxidation must also occur with the formation of $Ru_2(ap)_4(C{\equiv}CC_5H_4N)_2$ **1**. As earlier indicated, all previously synthesized $Ru_2(L)_4(C{\equiv}CC_6H_5)_2$ complexes retain the isomeric form of the starting $Ru_2(L)_4$ compound but this was not the case for **1**. Because $Ru_2(L)_4(C{\equiv}CC_6H_5)_2$ and **1** are both obtained via air oxidation, it is thus likely that the isomeric conversion of **1** occurs before the sample was exposed to air. The diruthenium complex (4,0) $Ru_2(F_3ap)_4Cl$ **2** was prepared by reacting (3,1) $Ru_2(F_3ap)_4Cl$ with excess TBACl·$H_2O$ (eq 2). Interestingly, the conversion of (3,1) $Ru_2(F_3ap)_4Cl$ to (4,0) $Ru_2(F_3ap)_4Cl$ is not observed when TBACl·$H_2O$ is replaced by TEACl in the experimental procedure. One plausible explanation is that TEACl is anhydrous and that water may be required; however, there was also no isomeric conversion when water had been added to a $CH_2Cl_2$ solution of (3,1) $Ru_2(F_3ap)_4Cl$, which had been left to react overnight with 0.5 M TEACl.

$$\text{(3,1) } Ru_2(F_3ap)_4Cl \xrightarrow{\text{excess TBACl·H}_2O} \text{(4,0) } Ru_2(F_3ap)_4Cl \quad (2)$$

**Molecular Structure. 1** crystallizes in the monoclinic unit cell with space group $P2_1/n$. The *ORTEP* diagram of **1** is illustrated in Figure 1, whereas selected bond lengths and bond angles of the compound are summarized in Table 2. The *ORTEP* diagram of **1** shows that the compound has four ap ligands in an equatorial position and two $C{\equiv}CC_5H_4N^-$ anions in axial positions, the latter of which are bound to the ruthenium atom via the terminal carbon of the acetylide group to complete a square-pyramidal geometry for both Ru1 and Ru2. As illustrated in Figure 1, Ru1 is coordinated to three pyridyl nitrogen atoms, one anilino nitrogen atom, and one axial carbon atom, whereas Ru2 is coordinated to one pyridyl nitrogen atom, three anilino nitrogen atoms, and one axial carbon atom. The structural data in Figure 1 shows that **1** adopts a (3,1) isomeric conformation, indicating that an isomeric transformation has occurred upon reaction with (4,0) $Ru_2(ap)_4Cl$. Remarkably, this is the only reported example of a $Ru_2$ complex bridged by four ap ligands, which exists in a (3,1) isomeric form. The Ru−Ru bond length in **1** is 2.4543(5) Å, and this value is much larger than the Ru−Ru bond length in the parent compound $Ru_2(ap)_4Cl$ (2.275(3) Å) (Table 3). Such an elongation of the Ru−Ru bond distance has already been reported upon conversion of $Ru_2(ap)_4Cl$ to the $Ru_2^{6+}$ complex, $Ru_2(ap)_4(C{\equiv}CC_6H_5)_2$ (where the Ru−Ru distance is 2.4707(8) Å). Other bond lengths of **1**, the parent compound $Ru_2(ap)_4Cl$, and $Ru_2(ap)_4(C{\equiv}CC_6H_5)_2$ for comparison purposes are given in Table 3.

The average Ru−$N_a$ ($N_a$ = anilino nitrogen) bond length in **1** (2.008Å) is shorter than that in $Ru_2(ap)_4(C{\equiv}CC_6H_5)_2$ (2.050 Å), whereas the opposite trend occurs for the average Ru−$N_p$ ($N_p$ = pyridyl nitrogen) bond length. This might be accounted for by the fact that **1** has a (3,1) isomeric form, whereas $Ru_2(ap)_4(C{\equiv}CC_6H_5)_2$ retains a (4,0) isomeric conformation; however, an isomeric effect on the average

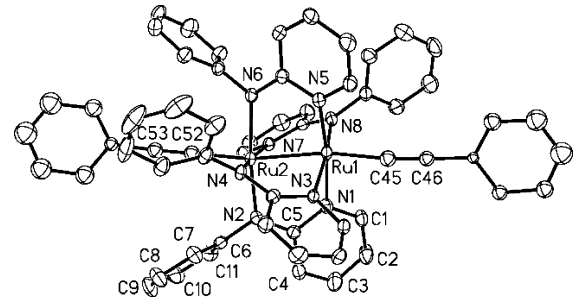


**Figure 1.** *ORTEP* diagram of (3,1) $Ru_2(ap)_4(C{\equiv}CC_5H_4N)_2$ **1**. Hydrogen atoms are being omitted for clarity.

**Table 2.** Selected Bond Lengths (Angstroms) and Bond Angles (Degrees) for (3,1) $Ru_2(ap)_4(C{\equiv}CC_5H_4N)_2$ **1**

| | | | |
|---|---|---|---|
| Bond Lengths (angstroms) | | | |
| Ru−Ru | 2.4543(5) | Ru−$C_{axial}$ | 1.96(2) |
| Ru−N1 | 2.085(4) | Ru−N5 | 2.037(4) |
| Ru−N2 | 2.003(4) | Ru−N6 | 2.064(4) |
| Ru−N3 | 2.172(4) | Ru−N7 | 2.175(4) |
| Ru−N4 | 1.985(4) | Ru−N8 | 1.977(4) |
| Bond Angles (degrees) | | | |
| Ru−Ru−N1 | 84.32(10) | Ru−Ru−$C_{axial}$ | 162.7(5) |
| Ru−Ru−N2 | 90.52(11) | Ru−C−C | 174(2) |
| Ru−Ru−N3 | 78.68(9) | C45−Ru−Ru-52 | 177(3) |
| Ru−Ru−N4 | 93.26(10) | N1−Ru−Ru-C52 | 104(3) |
| Ru−Ru−N5 | 88.81(11) | N1−Ru−Ru-N2 | 16.83(15) |
| Ru−Ru−N6 | 83.20(10) | N3−Ru−Ru-N4 | 26.42(15) |
| Ru−Ru−N7 | 78.81(10) | N5−Ru−Ru-N6 | 24.35(15) |
| Ru−Ru−N8 | 94.42(11) | N7−Ru−Ru-N8 | 22.05(15) |

**Table 3.** Selected Bond Lengths (Angstroms) and Bond Angles (Degrees) of (3,1) $Ru_2(ap)_4(C{\equiv}CC_5H_4N)_2$ **1**, (4,0) $Ru_2(ap)_4Cl$, and (4,0) $Ru_2(ap)_4(C{\equiv}CC_6H_5)_2$

| | (3,1) $Ru_2(ap)_4(C{\equiv}CC_5H_4N)_2$ **1** | (4,0) $Ru_2(ap)_4Cl$[41] | (4,0) $Ru_2(ap)_4(C{\equiv}CC_6H_5)_2$[30] |
|---|---|---|---|
| | Bond Lengths (angstroms) | | |
| Ru−Ru | 2.4543(5) | 2.275(3) | 2.4707(8) |
| $Ru-N_a$[a] | 2.008 | 2.026 | 2.050 |
| $Ru-N_p$[a] | 2.118 | 2.104 | 2.067 |
| Ru−X | 1.962 (X=$C_2C_5H_4N$) | 2.437 (X = Cl) | 1.988 (X=$C_2C_6H_5$) |
| | Bond Angles (degrees) | | |
| $Ru-Ru-N_a/N_p$[a] | 90.35/82.66 | 87.90/89.00 | 85.60/87.00 |
| Ru−Ru−X[a] | 167.2 (X=$C_2C_5H_4N$) | 180.0 (X = Cl), 162.4 (X = $C_2C_6H_5$) | |

[a] Averaged values.

$Ru-N_a$ and $Ru-N_p$ bond lengths was not seen when comparing the (3,1) and (4,0) isomers of $Ru_2(F_5ap)_4(C{\equiv}CC_6H_5)_2$.[23,30] The Ru−X bond length in **1** is 1.962 Å, a value similar to the Ru−X bond length in $Ru_2(F_5ap)_4(C{\equiv}CC_6H_5)_2$ (1.988 Å). In **1**, the average $Ru-Ru-N_a$ bond angle is greater than the average $Ru-Ru-N_p$ bond angle (Table 3). A different trend is seen in the case of $Ru_2(F_5ap)_4(C{\equiv}CC_6H_5)_2$, but this might be explained in terms of the change in isomeric form of the compound since other (3,1) isomers of $Ru_2(L)_4(C{\equiv}CC_6H_5)_2$ also possess an average $Ru-Ru-N_a$ bond angle, which is greater than the average $Ru-Ru-N_p$ bond angle. Finally, the Ru−Ru−C bond angle of **1** is 167.2°, a value close to the 161.0−164.3° values found in other (3,1) isomers of $Ru_2(L)_4(C{\equiv}CC_6H_5)_2$.[30]

**Electrochemistry of (3,1) $Ru_2(ap)_4(C{\equiv}CC_5H_4N)_2$ 1.** Part a of Figure 2 shows a cyclic voltammogram of **1** in $CH_2Cl_2$, 0.1 M TBAP whereas Table 4 summarizes half-wave potentials for each redox reaction of this compound along with data for (4,0) $Ru_2(ap)_4Cl$ and (4,0) $Ru_2(ap)_4(C{\equiv}CC_6H_5)_2$ under the same solution conditions. (3,1) $Ru_2(ap)_4(C{\equiv}CC_5H_4N)_2$ **1** undergoes one reversible oxidation and two reversible reductions, and this is also the case for (4,0) $Ru_2(ap)_4(C{\equiv}CC_6H_5)_2$.[30] The electron transfer processes of the newly synthesized **1** at $E_{1/2}$ = 0.69, −0.52, and −1.44 V are all metal-centered and assigned to the $Ru_2^{7+/6+}$, $Ru_2^{6+/5+}$, and $Ru_2^{5+/4+}$ redox couples, respectively. These assignments are based on what has been reported for related (3,1) and (4,0) derivatives of $Ru_2(L)_4(C{\equiv}CC_6H_5)_2$ where L = ap, Fap, $F_3$ap, or $F_5$ap[30] and are consistent with the potential separation between the first reduction and oxidation of **1** (1.21 V), which is virtually identical to the HOMO−LUMO gap of 1.23 V for the parent compound, (4,0) $Ru_2(ap)_4Cl$ (Table 4). The electroreduction process of **1** ($E_{1/2}$ = −1.44 V) is more than 200 mV easier than the electroreduction of (4,0) $Ru_2(ap)_4(C{\equiv}CC_6H_5)_2$ ($E_{pc}$ = −1.67 at 0.1 V/s), and this can be accounted for by the fact that the pyridyl groups decrease the electron density more on the diruthenium unit than do the phenyl groups.

**UV−Vis Spectroelectrochemistry of (3,1) $Ru_2(ap)_4(C{\equiv}CC_5H_4N)_2$ 1.** The UV−vis spectrum of **1** in $CH_2Cl_2$, 0.2 M TBAP before and after oxidation or reduction at a controlled potential is shown in part b of Figure 2. The initial compound has a major band at 607 nm and a weaker band at ∼1040 nm. This spectrum is similar to spectra of (3,1) or (4,0) $Ru_2(L)_4(C{\equiv}CC_6H_5)_2$ derivatives with substituted ap bridging ligands, which have bands at 622−623 and 1030−1031 nm under similar solution conditions. As the first oxidation of **1** proceeds (the $Ru_2^{6+/7+}$ process), the 607 nm band decreases in intensity and a broad low intensity band grows in between 400 and 1000 nm. These spectral changes contrast with what occurs upon oxidation of (3,1) or (4,0) $Ru_2(L)_4(C{\equiv}CC_6H_5)_2$[30] where the singly oxidized products are characterized by three well-defined absorption bands between 400 and 1000 nm. These differences might be accounted for by the different type of axial ligands, pyridyl vs phenyl.

The spectral changes during reduction of (3,1) $Ru_2(ap)_4(C{\equiv}CC_5H_4N)_2$ **1** at −0.8 V (the $Ru_2^{6+/5+}$ process) are also shown in part b of Figure 2. Like in the case of oxidation, the 607 and 1040 nm bands decrease in intensity during reduction as new bands grow in at 358, 530, and 820 nm. Similar UV−vis spectral changes are observed during the $Ru_2^{6+}/Ru_2^{5+}$ reaction of $Ru_2(ap)_4(C{\equiv}CC_6H_5)_2$.[30]

**Isomeric Change of (3,1) $Ru_2(F_3ap)_4Cl$ to (4,0) $Ru_2(F_3ap)_4Cl$ Monitored by Electrochemistry and UV−Vis Spectroscopy.** The stepwise addition of $TBACl{\cdot}H_2O$ to $CH_2Cl_2$ solutions containing (3,1) $Ru_2(F_3ap)_4Cl$ and 0.1 M TBAP results in a change in the electro-oxidation behavior, which initially depends upon the concentration of $Cl^-$ in solution and then, at higher concentrations of $Cl^-$, upon the time elapsed since the preparation of the solution. Three distinctly different half-wave potentials are observed for oxidation of (3,1) $Ru_2(F_3ap)_4Cl$ under the different experimental conditions (Figure 3). The one-electron oxidation of freshly prepared (3,1) $Ru_2(F_3ap)_4Cl$ in $CH_2Cl_2$ containing only 0.1 M TBAP is located at $E_{1/2}$ = 0.62 V, as reported in the literature[41] but immediately after adding high concentrations of $TBACl{\cdot}H_2O$ to solution the potential shifts negatively from 0.62 to 0.29 V. The same current−voltage curve is reproducibly obtained in $CH_2Cl_2$ with 1000 eq $TBACl{\cdot}H_2O$ upon multiple scans over 25−30 min but changes begin to occur at longer times as a new reversible redox process grows in at $E_{1/2}$ = 0.10 V, whereas currents for the process at 0.29 V decrease in magnitude.

In contrast to the oxidation, the potentials for reduction of (3,1) $Ru_2(F_3ap)_4Cl$ and/or its reaction products after addition of $TBACl{\cdot}H_2O$ remain relatively constant at about −0.65 V under all experimental conditions. This is consistent with earlier reports that the $Ru_2^{5+/4+}$ process of $Ru_2(L)_4Cl$ or $Ru_2(L)_4X$ compounds is independent of the isomer

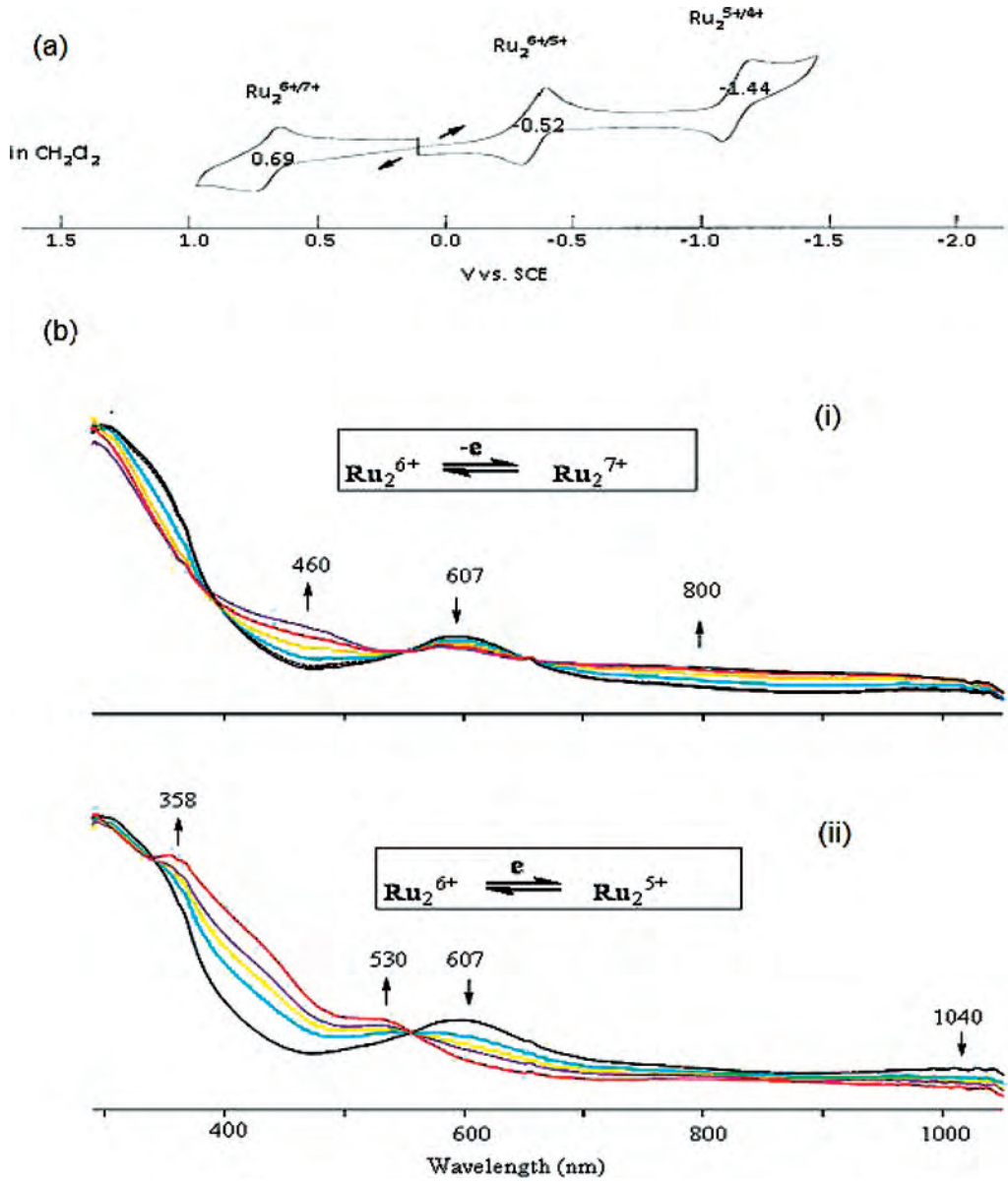


**Figure 2.** (a) Cyclic voltammogram of (3,1) $Ru_2(ap)_4(C{\equiv}CC_5H_4N)_2$ **1** in $CH_2Cl_2$, 0.1 M TBAP at a scan rate of 0.10 V/s and (b) UV−vis spectral changes of **1** in $CH_2Cl_2$, 0.2 M TBAP upon controlled potential (i) oxidation at $E_{app} = 1.0$ V and (ii) reduction at $E_{app} = -0.8$ V.

**Table 4.** Half-Wave Potentials for Redox Reactions of (4,0) $Ru_2(ap)_4Cl$,[41] (4,0) $Ru_2(ap)_4(C{\equiv}CC_6H_5)_2$,[30] and (3,1) $Ru_2(ap)_4(C{\equiv}CC_5H_4N)_2$ **1** in $CH_2Cl_2$, 0.1 M TBAP

| | | $E_{1/2}$ (V vs SCE) | | | |
|---|---|---|---|---|---|
| compound | ox state | $Ru_2^{7+/6+}$ | $Ru_2^{6+/5+}$ | $Ru_2^{5+/4+}$ | $\Delta^a$ |
| (4,0) $Ru_2(ap)_4Cl$ | $Ru_2^{5+}$ | ~1.33 | 0.37 | −0.86 | 1.23 |
| (4,0) $Ru_2(ap)_4$-$(C{\equiv}CC_6H_5)_2$ | $Ru_2^{6+}$ | 0.55 | −0.54 | −1.67[b] | 1.09 |
| (3,1) $Ru_2(ap)_4$-$(C{\equiv}CC_5H_4N)_2$ **1** | $Ru_2^{6+}$ | 0.69 | −0.52 | −1.44 | 1.21 |

[a] Potential gap in V between the $Ru_2^{6+/5+}$ and $Ru_2^{5+/4+}$ couples in the case of $Ru_2(ap)_4Cl$ and the $Ru_2^{7+/6+}$ and $Ru_2^{6+/5+}$ couples in the case of the other two compounds. [b] $E_{pc}$ at a scan rate of 0.1 V/s.

type[23,41] and also independent of the anionic axial ligand X, which usually binds weakly to $Ru_2^{5+}$, the only exception being in the case of $CN^-$.[24]

The invariance of $E_{1/2}$ for the processes at $E_{1/2} = 0.29$ in Figure 3 with changes in [$Cl^-$] is consistent with a mechanism where the neutral and singly oxidized forms of the electroactive compound have the same number of coordinated $Cl^-$ axial ligands.[51] The electrooxidation mechanism in each case can then only be described by eq 3 because the alternate possibility of a $Ru_2^{5+/6+}$ process involving $Ru_2(F_3ap)_4Cl$ and $[Ru_2(F_3ap)_4Cl]^+$ is only seen in the absence of added chloride.

$$(3,1)\ [Ru_2(F_3ap)_4Cl_2]^- \rightleftharpoons (3,1)\ Ru_2(F_3ap)_4Cl_2 + e^- \quad (3)$$

As will be described below, the change in the reversible potential from 0.29 to 0.10 V occurs only after an air oxidation of (3,1) $Ru_2(F_3ap)_4Cl_2$ at longer times and a following rearrangement of the bridging ligands on the singly oxidized species to give (4,0) $Ru_2(F_3ap)Cl_2$ which is in its $Ru_2^{6+}$ form.

(50) Lin, X. Q.; Kadish, K. M. *Anal. Chem.* **1985**, *57*, 1489.
(51) Crow, D. R. *Polarography of Metal Complexes*; Academic Press: London, 1969.

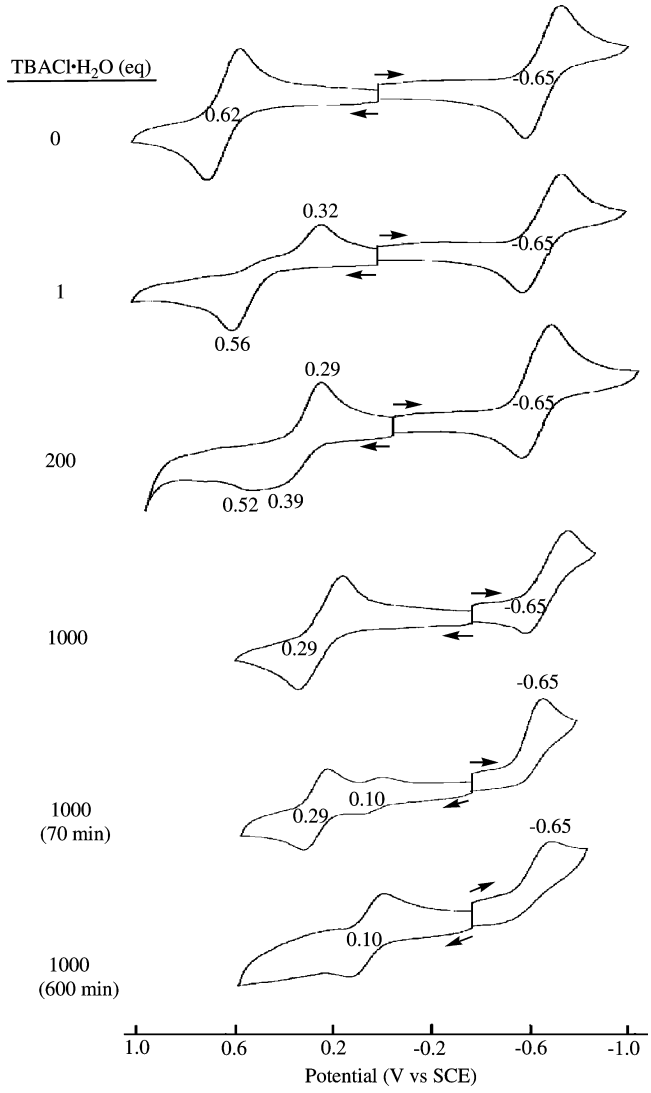


**Figure 3.** Cyclic voltammograms of (3,1) $Ru_2(F_3ap)_4Cl$ in $CH_2Cl_2$ with added $TBACl·H_2O$ and time-dependence in the presence of 1000 equiv $TBACl·H_2O$. Scan rate = 0.1 V/s.

Time-dependent changes are also observed in the UV−vis spectrum of the initial (3,1) $Ru_2(F_3ap)_4Cl$ complex as the (4,0) isomer is formed and this is shown in Figure 4. Immediately after addition of 1000 eq $TBACl·H_2O$ to solution, the UV−vis spectrum is characterized by three absorption bands at $\lambda_{max}$ = 418, 478, and 777 nm, a spectrum that closely resembles the UV−vis spectrum of (3,1) $Ru_2(F_3ap)_4Cl$ in neat $CH_2Cl_2$.[41] Over the first 25 min, the three absorption bands of the initial compound decrease slightly in intensity and a new shoulder peak develops at 895 nm. There are two isosbestic points at 615 and 816 nm, thus suggesting that over this time interval only two species are present in equilibria, the most likely of which are (3,1) $Ru_2(F_3ap)_4Cl$ and (3,1) $[Ru_2(F_3ap)_4Cl_2]^-$ on the basis of the electrochemical data that shows a reversible oxidation at 0.29 V, which is independent of $[Cl^-]$.

From 25 to 500 min, a more significant set of changes is observed in the UV−vis spectrum (Figure 4). Two new bands grow in at $\lambda_{max}$ = 446 and 580 nm, while, at the same time, the lower energy absorption band decreases significantly in intensity. There is an isosbestic point at 630 nm, again

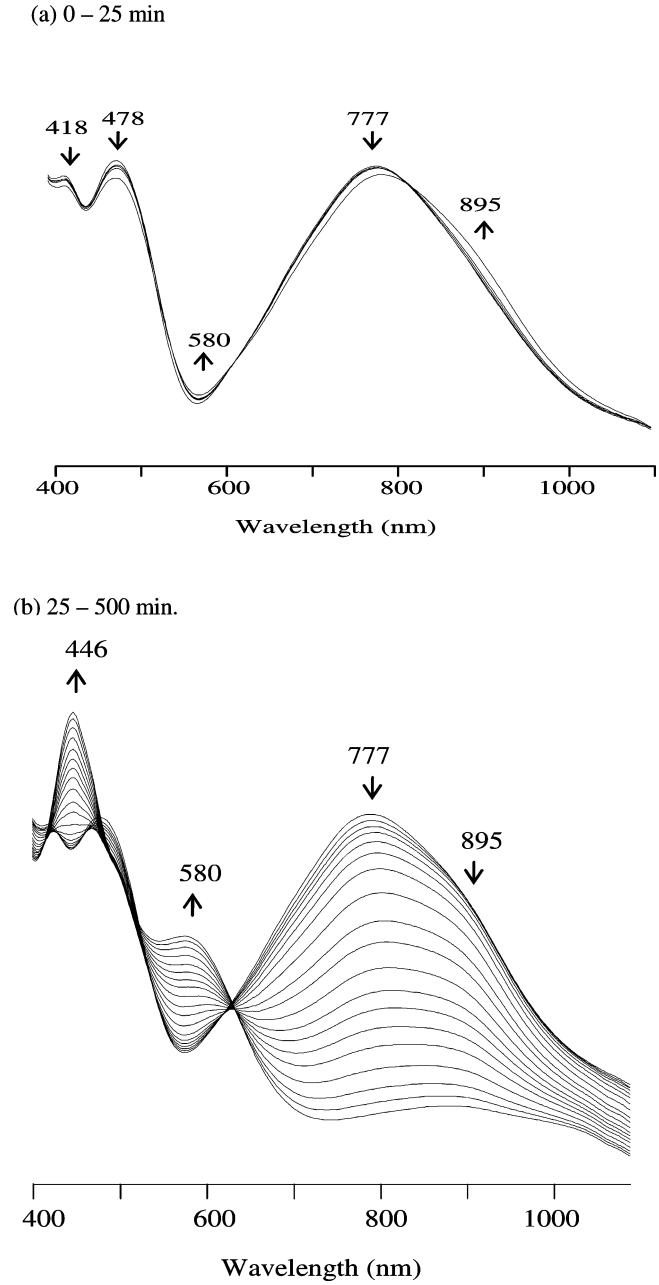


**Figure 4.** UV−vis spectral changes of (3,1) $Ru_2(F_3ap)_4Cl$ in $CH_2Cl_2$, 1000 equiv $TBACl·H_2O$ with respect to time for (a) time = 0−25 min and (b) 25−500 min.

suggesting that only two species are present in equilibrium from 25 to 500 min. The final spectrum after 500 min exhibits absorption bands at 446, 580, and 895 nm and is reminiscent of the 466, 634, and 895 nm bands for $Ru_2(F_3ap)_4(C{\equiv}CC_6H_5)_2$,[30] therefore suggesting that the final product contains a $Ru_2^{6+}$ core and further suggesting that the process at 0.10 V is not an oxidation of $Ru_2^{5+}$ but rather the reduction of a $Ru_2^{6+}$ species generated in solution. This is indeed the case, as demonstrated by rotating disk voltammograms of a similar solution obtained as a function of time. These voltammograms are shown in Figure 5 and parallel what is observed in the time-resolved electrochemical and spectroscopic measurements of (3,1) $Ru_2(F_3ap)_4Cl$ under the same solution conditions.

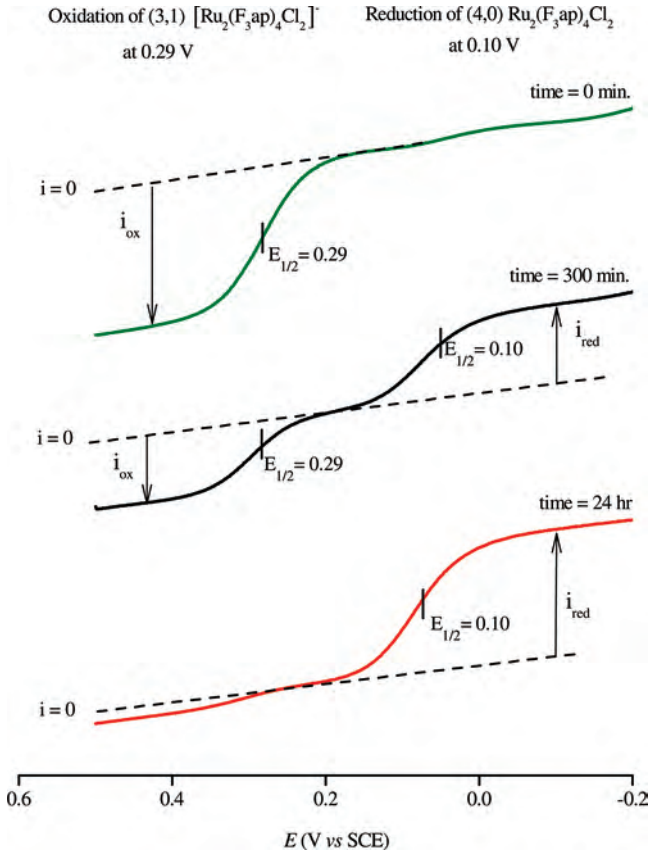


**Figure 5.** Rotating disk voltammograms of (3,1) $Ru_2(F_3ap)_4Cl$ in $CH_2Cl_2$ containing 0.1 M TBAP and 1000 equiv $TBACl \cdot H_2O$ immediately after solution preparation ($t = 0$ min) and after 5 or 24 h of elapsed time. Rotation rate = 1600 rpm.

**Scheme 1.** Conversion of (3,1) $Ru_2(L)_4Cl$ to (4,0) $Ru_2(L)_4Cl$ in $CH_2Cl_2$ Solutions Where L = $F_3ap$[a]

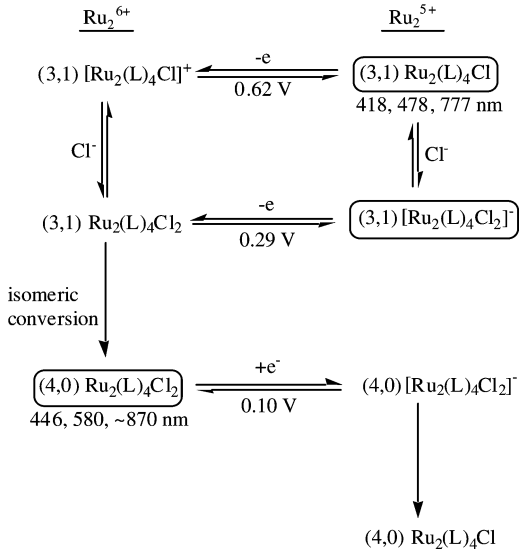


[a] The initial oxidation of (3,1) $Ru_2(L)_4Cl$ or (3,1) $[Ru_2(L)_4Cl_2]^-$ converts to a reduction of (4,0) $Ru_2(L)_4Cl_2$ after >10 hrs in the presence of $TBACl \cdot H_2O$.

One key advantage of the RDE measurement is its ability to uniquely differentiate an oxidation from a reduction reaction, the former having maximum limiting diffusion currents below the $i = 0$ line and the later having currents above the $i = 0$ line, both of which will increase with the square root of rotation rate, $\omega^{1/2}$, for diffusion-controlled electron transfer processes.[52] As seen in Figure 5, the RDE response of a freshly prepared (3,1) $Ru_2(F_3ap)_4Cl$ solution in the presence of high $[Cl^-]$ (top green curve in Figure 5) is that for a reversible electrooxidation at $E_{1/2} = 0.29$ V. A plot of the maximum peak current versus $\omega^{1/2}$ (Figure S1 in the Supporting Information) is linear, consistent with the transfer of 1.0 electron to give the singly oxidized species and no other redox processes are observed between −0.2 and +0.6 V versus SCE.

The solution of (3,1) $Ru_2(F_3ap)_4Cl$ was then left to stand for 5 h and the RDE measurements repeated (black curve in Figure 5). Under these conditions, the maximum oxidation currents for the process at $E_{1/2} = 0.29$ V decrease by about 50% and a new reversible reduction process is observed at $E_{1/2} = 0.10$ V. This parallels what is seen in Figure 3 and indicates an approximately equimolar mixture of the (3,1) $Ru_2(F_3ap)_4Cl$ isomer (in its bis-chloride form) and the newly generated $Ru_2^{6+}$ product, the latter being formulated as (4,0) $Ru_2(F_3ap)_4Cl_2$ on the basis of the spectroscopic and electrochemical data and a structural characterization of the isolated reaction product after workup (Experimental Section).

Finally, after 24 h in solution, there is a nearly complete conversion of (3,1) $Ru_2(F_3ap)_4Cl$ to its singly oxidized (4,0) isomer and the RDE (red line in Figure 5) is then characterized by a reduction at $E_{1/2} = 0.10$ V with little to no oxidation currents at the more positive potential of 0.29 V. This is again consistent with what is observed by electrochemistry and UV−vis spectroscopy under the same solution conditions. The maximum current for reduction of the homogeneously generated species in solution, formulated as (4,0) $Ru_2(F_3ap)_4Cl_2$, is proportional to the square root of the rotation rate indicating diffusion control and the number of electrons transferred is calculated as $n = 1$ on the basis of a Levich plot shown in Figure S1 in the Supporting Information.

The $Ru_2^{6+}$ form of the diruthenium compound formed upon air oxidation is stable in solution for several days but all attempts to isolate this oxidized species for further characterization led only to a final product which was structurally characterized as (4,0) $Ru_2(F_3ap)_4Cl$ (Experimental Section). The X-ray structure of the isolated product is identical to that which was earlier published for (4,0) $Ru_2(F_3ap)_4Cl$ synthesized by another method.[41] Electrochemical and spectroscopic properties of previously characterized (4,0) $Ru_2(F_3ap)_4Cl$ also match the properties of the product isolated and structurally characterized after air oxidation of (3,1) $Ru_2(F_3ap)_4Cl$ in $CH_2Cl_2$ containing $TBACl \cdot H_2O$. Thus electrochemical, spectroscopic, and structural data are self-consistent and proposed reaction pathways for the conversion of (3,1) $Ru_2(F_3ap)Cl$ to (4,0) $Ru_2(F_3ap)_4Cl$ are summarized in Scheme 1, where species in solution are indicated by a box around the formula and the other species are generated at the electrode surface.

(52) Bard, A. J.; Faulker, L. R. *Electrochemical Methods: Fundamentals and Applications*; John Wiley & Sons: New York, 2000; 2nd Edition.

It was earlier reported that only small differences are observed between the $Ru_2^{5+/6+}$ processes of (3,1) and (4,0) $Ru_2(F_3ap)_4Cl$ in noncoordinating media, $E_{1/2}$ values for electrooxidation being 0.62 and 0.69 V, respectively, in $CH_2Cl_2$.[41] Much larger differences in $E_{1/2}$ are seen for the $Ru_2^{6+/5+}$ process of (3,1) $Ru_2(F_3ap)_4Cl_2$ and (4,0) $Ru_2(F_3ap)_4Cl_2$, and this can be accounted for by structural differences between the two diruthenium compounds, which leads to different strengths of axial coordination to the $Ru_2^{5+}$ form of the two isomers.

In summary, we have shown two examples of isomeric conversions among diruthenium complexes. One type of isomeric conversion involves a change in configuration from (4,0) to (3,1) and is observed when (4,0) $Ru_2(ap)_4Cl$ reacts with $LiC{\equiv}CC_5H_4N$. The other isomeric change involves a conversion of (3,1) $Ru_2(F_3ap)_4Cl$ to (4,0) $Ru_2(F_3ap)_4Cl$ in the presence of excess $TBACl{\cdot}H_2O$. The fact that (4,0) $Ru_2(F_3ap)_4Cl$, a minor product in the reaction between $Ru_2(CH_3CO_2)_4Cl$ and $HF_3ap$, can be subsequently formed as the sole product isolated from the major (3,1) isomer, thus eliminating the need for a time-consuming and costly separation process to obtain the (4,0) isomer, which can then be further studied as to its reactivity.

**Acknowledgment.** Support from the Robert A. Welch Foundation (J.L.B., Grant E-918; K.M.K., Grant E-680) is gratefully acknowledged. T.P. acknowledges support from a TSU Seed Grant and a Departmental Welch Grant. We also thank Dr. J. D. Korp for X-ray analyses.

**Supporting Information Available:** X-ray crystallographic data for compound **1** (CIF format) and Levich plots from RDE data for the $Ru_2^{5+/6+}$ reactions of the (3,1) and (4,0) isomers. This material is available free of charge via the Internet at http://pubs.acs.org.

IC800787P